Acta Cryst. (1995). B51, 81–89

The Inclusion Compound of Deoxycholic Acid with (–)-Camphor: a Structural and Energetic Study

BY SOFIA CANDELORO DE SANCTIS

Facolta' di Medicina, Dipartimento di Chimica, Universita' di Roma 'La Sapienza', Piazzale A. Moro 5, 00185 *Roma, Italy*

AND VINCENZA M. COIRO, FERNANDO MAZZA AND GIORGIO POCHETTI

Istituto di Strutturistica Chimica 'Giordano Giacomello' del CNR, CP No. 10, 00016 *Monterotondo Stazione, Roma, Italy*

(*Received* 8 *March* 1994; *accepted* 15 *July* 1994)

Abstract

The crystals of the 2:1 inclusion compound of deoxycholic acid (3α,12α-dihydroxy-5β-cholan-24-oic acid) with (–)-camphor are orthorhombic, space group $P2_12_12$, with a = 27.266 (4), b = 13.865 (2), c = 7.237 (1) Å, Z = 4 ($C_{24}H_{40}O_4.0.5C_{10}H_{16}O$)/unit cell. The final R value is 0.075 for the 2155 reflections with $I > 1.5\sigma(I)$. The deoxycholic acid molecules are held together by a network of hydrogen bonds into pleated bilayers. The (–)-camphor molecules occupy channels with apolar surfaces arising from the packing of the bilayers. The channels have an approximate square cross section, very similar to that of the previously determined crystal structure of the inclusion compound with (+)-camphor. The (–)-camphor molecule was located by potential-energy calculations. Six different sites of camphor were found, satisfactory from the energy point of view. The presence of at least three of them in the crystals was confirmed by difference Fourier syntheses and least-squares refinement techniques. The host–guest interaction properties are similar for the (+)- and (–)-camphor inclusion compounds, therefore, the optical isomer separation capability of the deoxycholic acid host lattice for camphor is not to be expected.

Introduction

Deoxycholic acid (3α,12α-dihydroxy-5β-cholan-24-oic acid, DCA, Fig. 1) is one of the components of the bile acids pool, the salts of which are responsible for many important biophysiological functions in bile and in the gastrointestinal apparatus. They are involved in solubilization, transport and absorption processes, interacting with molecules like cholesterol, fatty acids and bilirubin IXα. They also take an important part in the process of formation and solubilization of gallstones (Higuchi, 1984; Holzbach, 1984; Hostrow, 1984; Angelico, Candeloro De Sanctis, Gandin & Alvaro, 1990). The full interpretation of their activity at molecular level requires the knowledge of the possible interaction schemes and sites of these molecules among themselves and with those of the surrounding medium.

The study of deoxycholic acid inclusion compounds starts with the isolation from the liver of some animals of a crystalline material recognized to contain molecular complexes of deoxycholic acid and various kinds of fatty acids (Wieland & Sorge, 1916). Because of the biological interest of such compounds, investigations were carried out and, as soon as the X-ray analysis technique became suitable for problems of such complexity, the first attempts were made for the crystal structure solution (see, for example, Giacomello & Kratky, 1936).

The first crystal structures were solved in 1972 (Candeloro De Sanctis, Giglio, Pavel & Quagliata, 1972; Craven & De Titta, 1972) and the type of molecular packing (Figs. 2*a* and 2*b*), where the DCA molecules act as a host chiral network capable of 'including' the guest component, suggested a wide range of applications in chemistry other than in biology, bringing additional interest to this class of compounds. In the following years DCA was tested and used for stereospecific photoaddition reactions (Popovitz-Biro, Tang, Chang, Lahav & Leiserowitz, 1985; Padmanabhan, Venkatesan & Ramamurthy, 1987; Weisinger-Lewin *et al.*, 1987), photochemical reactions (Coiro, Giglio, Mazza & Pavel, 1984), inclusion stereoselective polimerization (Miyata & Takemoto,

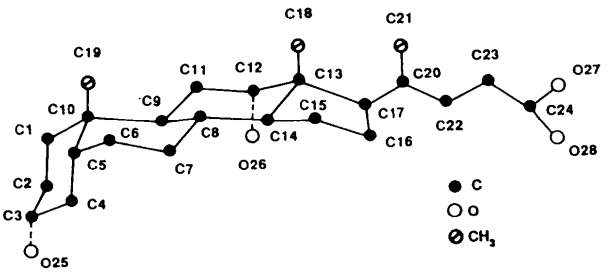

Fig. 1. Atomic numbering of DCA. H atoms are omitted.

1975; Audisio, Silvani & Zetta, 1984) and separation chemistry (Makin, 1975).

In the course of such studies, more than 40 crystal structures have been solved. Apart from very few examples of hexagonal (Candeloro De Sanctis *et al.*, 1978; Candeloro De Sanctis, Giglio, Petri & Quagliata, 1979) and tetragonal assemblies (Coiro, D'Andrea & Giglio, 1979; Tang, Popovitz-Biro, Lahav & Leiserowitz, 1979) with polar host–guest interactions, most of the inclusion compounds of DCA are orthorhombic, belonging to space groups $P2_12_12_1$ or $P2_12_12$. In all of them the DCA molecules are arranged, through an efficient network of hydrogen bonds, into pleated bilayers which pack together so that channels with apolar surfaces are formed (Fig. 2)

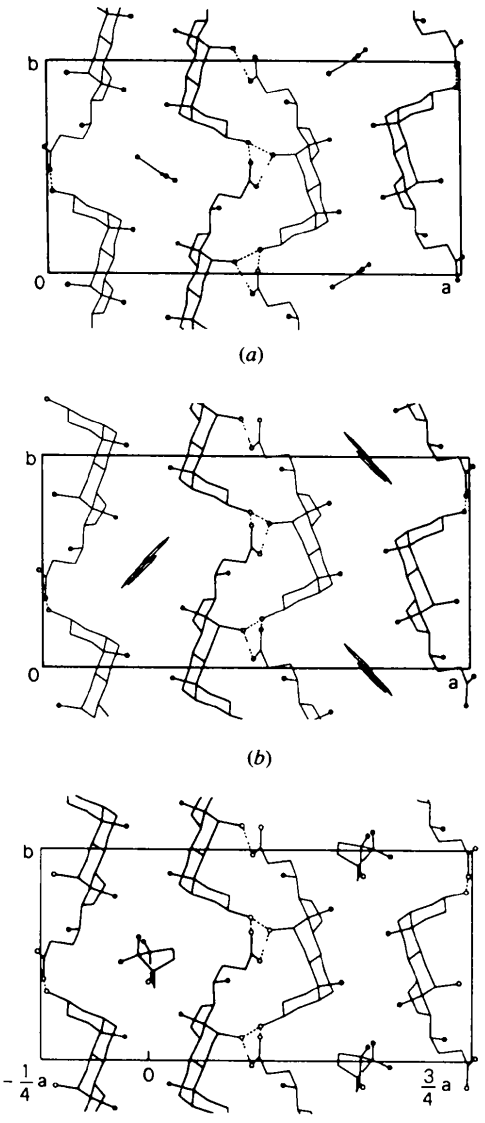

Fig. 2. Crystal structures of DCA, with guest molecules (*a*) acetone (Craven & De Titta, 1972), (*b*) phenanthrene (Candeloro De Sanctis, Giglio, Pavel & Quagliata, 1972) and (*c*) (+)-camphor (Jones, Schwarzbaum, Lessinger & Low, 1982), illustrating the three energetically stable cavities. The black and open circles are methyl groups and O atoms, respectively. The dotted lines are hydrogen bonds. H atoms are omitted.

The structure of the bilayers remains almost identical in all crystals, whereas the channels have different size and shape according to the relative position of the double layers. They can thus accommodate molecules of different steric and electronic properties, mostly of apolar nature (for a full discussion, see Giglio, 1984; Popovitz-Biro, Tang, Chang, Lahav & Leiserowitz, 1985).

Some calculations of the potential energy of interaction between adjacent double layers indicated that only three relative positions are energetically stable (Candeloro De Sanctis & Giglio, 1979). This result has been widely confirmed experimentally, because all the crystal structures known so far belong to these three energy minima (with sometimes minor adjustments that optimize the interactions with the guest molecules). The three types of cavities corresponding to the three different energy minima are shown in Fig. 2.

The energetical stability of the cavities and the knowledge of their possible size and shape make DCA suitable for problems of molecular recognition and allow some chemical engineering to be performed with rather accurate prediction of the molecules which can enter and best fit the different kinds of cavities.

In some early literature (Baron, 1961) the capability of DCA to separate optically active isomers had been tested and it was reported to be promising for camphor, with a preference for (–)-camphor (LCP).

The crystal structure of the DCA inclusion compound with (+)-camphor (DCADCP) had been studied (Jones, Schwarzbaum, Lessinger & Low, 1982; Fig. 2*c*) and potential-energy calculations, together with careful inspection of the Fourier maps, had shown that the (+)-camphor molecule (DCP) occupied more than one site, each having specific interactions with the host lattice, mainly through the methyl groups and H atoms (Candeloro De Sanctis, Chiessi & Giglio, 1985). With this information and the present knowledge of the properties of the DCA cavities, it was not possible to predict any selectivity. Therefore, we carried out a parallel study for the DCA–(–)-camphor inclusion compound (DCALCP) in order to find out whether and why such selectivity occurred.

Experimental and structure solution

Colourless crystals in the form of elongated prisms were obtained at room temperature on slow evaporation from an ethanolic solution where the DCA was dissolved together with LCP in slight excess with respect to the expected stoichiometric 2:1 ratio of DCA/LCP.

On heating the crystals showed some loss of camphor between 423 and 428 K, without loss of birefringence, until complete fusion occured at 447 K. This value has to be compared with the reported DCADCP melting point of 448 K. Crystal data and the data collection procedure are reported in Table 1, where some comparative values for DCADCP are also reported.

The identity of the space group and the close similarity of the cell dimensions between DCALCP and DCADCP were a strong indication for an isomorphism between at least the DCA host lattices of the two crystal structures. The DCA molecules were then located refining the coordinates of DCA found in DCADCP through iterative Fourier syntheses followed by five cycles of full-matrix least squares using unit weights and isotropic temperature factors (see Table 1 for refinement procedure also).

At the end of this refinement the R factor was 0.20 for 2155 reflections with $I > 1.5\sigma(I)$ and the location of the DCA molecules was satisfactory. The success of this kind of procedure confirmed that the two structures, DCALCP and DCADCP, were very similar. The packing of the DCA molecules within the double layers is the same in both compounds and almost identical to that of all the other known orthorhombic crystal structures. The DCA molecules have the same side-chain conformation and the same intermolecular hydrogen-bonding scheme (see, for example, Giglio, 1984; Candeloro De Sanctis, Giglio, Petri & Quagliata, 1979, for a full description of the double layer). Further, the size and shape of the cavity was very similar to that of DCADCP (Fig. 2*c*) and of the other known crystal structures belonging to the same space group $P2_12_12$ (Padmanabhan, Venkatesan & Ramamurthy, 1984, 1987; Miki, Kasai, Tsutsumi, Miyata & Takemoto, 1987). A Fourier map calculated at this stage showed a region of unresolved electron density inside the channels. This was partly expected because of a twofold axis running through the camphor molecule, but the smeared electron density with the highest peak value of 1.8 e Å^{-3} (value to be compared with ~1.9 e Å^{-3} in DCADCP), indicated a similarity between the two structures, with LCP assuming different non-equivalent positions in the crystal. As in DCADCP, this was confirmed by potential-energy calculations and difference Fourier maps.

Potential-energy calculations

Semi-empirical atom–atom potentials were used in the form

$$V(r) = a\exp(-br)/r^d - c/r^6,$$

with the coefficients reported in the paper by Pavel, Quagliata & Scarcelli (1976) verified in known and unknown crystal structures. The methyl group was treated as one atom and a cut off distance of 7 Å was used for the interactions.

Table 1. *Summary of crystal data, data collection, solution and refinement details*

DCADCP data are given in square brackets for comparison.

Crystal data	
Chemical formula	$C_{24}H_{40}O_4.0.5C_{10}H_{16}O$
Molecular weight	468.6
Crystal system	Orthorhombic
Space group	$P2_12_12$ [$P2_12_12$]
a (Å)	27.266 (4) [27.353 (3)]
b (Å)	13.865 (2) [13.814 (2)]
c (Å)	7.237 (1) [7.233 (1)]
V (Å^3)	2735.9 (7)
Z	4
$F(000)$	1032
D_x (g cm^{-3})	1.138
No. of reflections for cell parameters	15
2θ range for cell parameters (°)	25–60
μ (cm^{-1})	5.14
Temperature (K)	293
Crystal form	Elongated prisms
Crystal size (mm)	0.2 × 0.4 × 0.5
Crystal colour	Colourless
Melting point (K)	447 [448]
Data Collection	
Diffractometer	Syntex P21
Scan type	$\theta/2\theta$ scans
Scan rate (min^{-1})	29.3–1.2
Radiation	Cu $K\alpha$
Absorption correction	From φ-scan curve of 2 reflections
No. of measured reflections	3400
No. of observed reflections	2155
Observation criterion	$I > 1.5\sigma(I)$
θ_{max} (°)	70
No. of standard reflections	3 every 100 reflections
Intensity variation	Small but steady decay
Refinement	
Structure solution	Full-matrix least squares
Final R	0.075
Final wR	0.083
No. of reflections used	2155
Weighting	
At beginning	$\sum w(\|F_o\| - \|F_c\|)^2, w = 1$
During later stages (G variable)	$w = K[\sigma^2(F_o) + GF_o^2]^{-1}$
Final K	1.43
Final G	0.002
Source of atomic scattering factors	Cromer & Mann (1968)
Computer program used	*SHELX*76 (Sheldrick, 1976)

For parallel calculations on different models: DCA: 15 cycles of isotropic followed by 16 cycles of anisotropic least-squares refinement. H atoms were generated at the expected positions with *SHELX*76 and kept riding on the bonded C atom with the same temperature factor in the isotropic cycles and temperature factor equal to U_{11} of the bonded C atom in the anisotropic cycles. The H atoms bonded to the two hydroxyl and the carboxyl O atoms were omitted in the refinement because their positions are not completely determined and their contribution would, however, be very low.

Camphor: refined throughout as rigid body with individual variable temperature factors, unless otherwise stated.

The atomic coordinates for DCA were kept fixed as obtained at the end of the isotropic least-squares refinement of DCA only (Table 1, deposited material).*

* Atomic coordinates of the DCA molecule, the LCP molecule, DCA atoms, H atoms, interatomic distances and angles of DCA, anisotropic displacement factors and structure factors have been deposited with the IUCr (reference NA055). Copies may be obtained through The Managing Editor, International Union of Crystallography, 5 Abbey Square, Chester CH1 2HU, England.

We calculated the van der Waals potential energy for the interactions of the LCP molecule with the DCA lattice and neighbouring LCP molecules as a function of three Eulerian angles of rotation, ψ_1, ψ_2 and ψ_3, of the rigid LCP molecule around three axes parallel to **a**, **b** and **c**, running through the centre of mass of the LCP molecule, and three translations t_x, t_y, t_z, along **a**, **b** and **c**. The calculation procedure consisted in a grid-point exploration of all the allowed parametric space, progressively reducing the angular increments from 10 to 2° and the translations from 0.4 to 0.1 Å, with the same method used for DCADCP (Candeloro De Sanctis, Chiessi & Giglio, 1985).

The model for LCP, reported in Fig. 3, was derived from the crystal structure of (–)-camphoroxime (Baert & Fouret, 1978), an accurate crystal structure with two independent molecules in the asymmetric unit, of which that with the lower temperature factors was chosen. H atoms were generated geometrically (C—H = 1.08 Å, H—C—H = 109.5°) and the O atom was positioned along the C—N bond, at the same distance used for DCP (1.18 Å).

Because of the close similarity of the cell dimensions and the positions of the DCA molecules in the crystals of DCADCP and DCALCP, we obtained the starting position for LCP bringing the LCP molecule to best overlap with DCP in its starting position in DCADCP. This was obtained with a best-fitting calculation (Gavuzzo, Pagliuca, Pavel & Quagliata, 1972) of all C atoms, except C2 and C6, which exchange their role in the two different stereoisomers. The starting atomic coordinates for LCP have been deposited (Table 2, deposited material).*

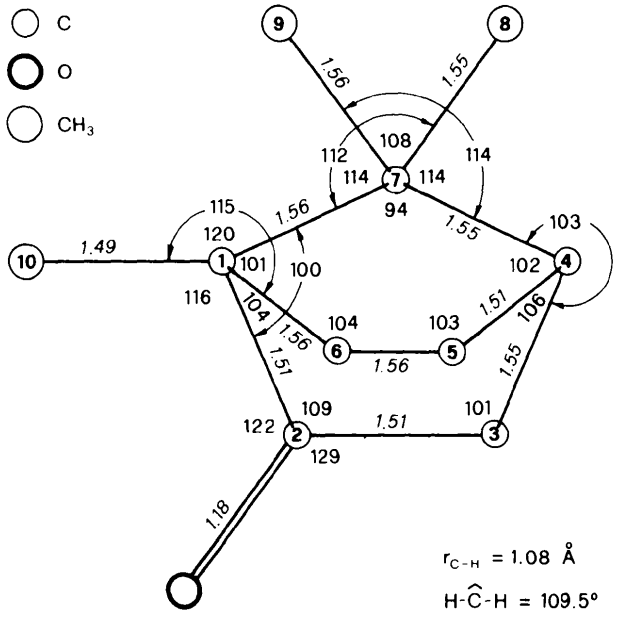

Fig. 3. Atomic numbering, bond lengths (Å) and angles (°) for the model of LCP.

Table 2. *Eulerian angles* (°), *translations* (Å) *and energy values* (kJ mol^{-1}) *corresponding to the van der Waals energy minima for LCP in DCALCP*

Minimum		ψ_1	ψ_2	ψ_3	t_x	t_y	t_z	E
A	*T*	195	48	73	−1.0	−0.1	0.1	−106.6
	R	209	50	57	−0.9	−0.1	0.2	−105.8
B	*T*	23	128	47	−0.2	0.9	0.1	−105.8
	R	29	128	47	−0.2	0.9	0.1	−105.3
C	*T*	210	30	144	−0.1	0.0	−0.3	−104.9
	R	208	51	149	0.1	0.3	−0.1	−103.2
D		325	130	262	−0.1	0.3	−0.7	−103.2
E		121	18	311	0.1	0.8	0.3	−103.2
F		242	100	228	−0.4	0.7	−0.2	−102.8

The six-dimensional potential-energy map showed six minima (Table 2), corresponding to positions in which there are good specific interactions between DCA and LCP (Table 3). The calculations were at first carried out taking into account the LCP–DCA interactions only. Later the interactions with adjacent camphor molecules were included, and two sets of calculations had to be performed owing to the space-group symmetry and the actual position of the camphor molecules on the twofold axis.

Type *T*: the adjacent molecules were related by a *c*-axis translation only.

Type *R*: the adjacent molecules were related by a *c*-axis translation and rotation of 180° around **c**.

For the first set of calculations (*T*) the final positions of LCP were almost unchanged, due to rather long and, therefore, irrelevant LCP–LCP contacts. For some of the *R*-type minima the molecule had t · readjust its position slightly because of a rather short contact with its first-neighbour LCP molecules. We checked this variation for the three deepest minima and found that the final energy values were very similar and the positional parameters (Table 2) had small differences which would not, however, affect the refinement procedure. Therefore, we did not repeat the minimization procedure for the remaining positions and considered only the *T* minima for further calculations.

The close similarity of the values of the six energy minima, ranging from −106.6 to −102.8 kJ mol^{-1} indicated that, at least in principle, the camphor molecule could occupy different positions inside the crystal channels. On the basis of the intermolecular distances (Table 3) and the energy values, none of the six positions corresponding to the energy minima could be discarded in the crystals. However, the three minima with the lowest energy were to be preferred because on the Fourier map calculated at the end of the refinement of DCA only the highest peaks in the LCP region corresponded to some of the atomic positions of the LCP molecule in those three minima. In Fig. 4 a typical

* See deposition footnote.

Table 3. *Closest intermolecular distances* (Å) *between DCA and LCP in DCALCP for the positions of LCP corresponding to the energy minima*

The H atoms have the same numbering as the C atoms to which they are bonded

	DCA asymmetric unit	DCA	LCP	Distance		DCA asymmetric unit	DCA	LCP	Distance
A	2	H16	C10	3.2	*B*	1	H6	C9	3.1
	2	H16	H6	2.3		2	H16	H6	2.3
	2	H22	H6	2.4		3	H16	C8	3.1
	3	H16	H3	2.4		3	H22	H3	2.3
	3	H22	C8	3.0		4	H6	H'5	2.2
	5	C19	H'3	3.0		5	C19	C8	3.8
	5	H'1	H'5	2.3		6	H20	C10	2.9
	6	C18	C9	3.8		7	C18	C8	3.7
	7	C18	H3	3.1		7	H20	O	2.7
	8	C19	C9	3.9					
C	1	H6	H6	2.2	*D*	2	H6	C9	3.1
	2	H16	C8	3.2		2	H22	C8	3.1
	2	H16	C10	3.0		3	H16	H'6	2.2
	2	H20	C10	2.9		3	H22	H'6	2.2
	3	H16	H'6	2.3		5	C19	O	3.5
	3	H22	H'3	2.3		6	C18	C9	3.7
	6	C18	C8	3.8		7	C18	C10	4.0
	6	C21	C9	4.0		7	C18	O	3.4
	7	C18	H'5	3.1		7	H20	C10	3.1
E	1	H6	C9	3.0	*F*	1	H6	C10	3.2
	2	H16	C10	3.0		2	H16	H3	2.4
	2	H16	O	2.7		2	H22	C8	2.9
	3	H16	H6	2.2		3	H16	C10	3.0
	3	H22	H6	2.4		3	H15	C10	3.1
	3	H22	C6	2.9		5	C19	C10	3.7
	5	C19	C9	3.9		5	H'1	C8	3.2
	7	C21	H5	3.1		6	H20	C9	3.2
	8	H5	H'3	2.1		7	C18	C10	3.7
						8	H'1	H'5	2.4

Equivalent positions: 1, x, y, z; 2, $x, y+1, z$; 3, $-x, -y, z$; 4, $-x, -y+1, z$; 5, $x, y, z+1$; 6, $x, y+1, z+1$; 7, $-x, -y, z+1$; 8, $-x, -y+1, z+1$.

section of the Fourier map in the region of the camphor molecule is reported, with the indications of some atoms belonging to the three models corresponding to the three deepest minima.

Least-squares refinement

The three 'best' models were at first introduced separately in three parallel least-squares refinement calculations carried out with the procedure reported in Table 1. The camphor molecule was introduced with an occupancy factor of 0.5, according to the stoichiometry of the complex.

The refinement of molecule *B* gave the lowest value of the disagreement index ($R = 0.087$) and more uniform values of the displacement factors of LCP (Table 4). The scattering among the values of the displacement factors in this kind of problem is too wide to be interpreted in terms of differences among the vibration amplitudes: it is rather a consequence of the presence of multiple molecular sites in the crystals. Therefore, the degree of uniformity of the displacement parameters at the end of a refinement is related to the reliability of the model and to the degree of overlapping with other models (Candeloro

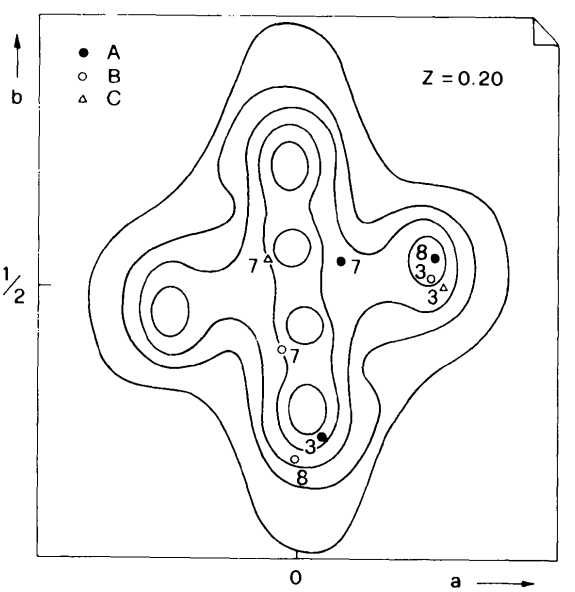

Fig. 4. A section of the difference electron-density map in the region of the camphor molecule, calculated at the end of the isotropic refinement of DCA only. Contour lines at intervals of 0.3 e Å^{-3} starting from 0.2 e Å^{-3}. Atoms of different models, sited within $z = \pm 0.03$ are plotted. The numbers refer to the corresponding C atoms.

Table 4. *Displacement parameters U* ($Å^2 \times 10^2$) *of the LCP atoms at the end of the single model refinements*

	A		*B*		*C*	
	Iso	Aniso	Iso	Aniso	Iso	Aniso
	(R=0.128)	(R=0.096)	(R=0.118)	(R=0.087)	(R=0.135)	(R=0.105)
	U		*U*		*U*	
C1	21	23	18	19	16	16
C2	18	18	21	21	16	16
C3	13	13	19	20	16	16
C4	19	22	26	29	28	28
C5	13	13	16	19	26	32
C6	16	15	21	21	17	21
C7	28	29	15	18	35	39
C8	27	26	16	18	14	17
C9	33	40	25	33	24	26
C10	40	43	28	27	38	44
O	39	53	46	48	36	39

De Sanctis, Chiessi & Giglio, 1985). However, each difference Fourier map calculated at the end of the three refinement calculations showed, in the channels, regions of positive electron density where many of the residual peaks were corresponding to atomic positions of the other models. These positive regions were more pronounced in the maps calculated with molecules *A* or *C*. These findings were a strong indication of the presence of the three models, with a higher population of *B* molecules in the crystals.

We then tried to push the refinement further, introducing two models in the calculations, in the attempt to match the electron-density map with an atomic distribution as near as possible to the actual situation in the crystals. We started with models *A* and *B*, which had the lowest *R* values in the single model refinements.

The results of the first set of cycles, carried out with an occupation factor of 0.25 for each model, appeared to still give some physically meaningful indications, because the displacement factors of *B* were on average lower than those of *A*, in agreement with our expectation that *B* had a higher occupancy in the crystals. Further, the agreement index dropped to 0.076, while a parallel calculation using the *A* and *C* models gave a higher *R* value (0.086) and worse displacement factors. Therefore, we did not carry out any further calculations for *A* + *C* and carried out a new set of refinement cycles for *A* + *B*, refining the occupancy factors. The displacement factors were kept fixed to the following values: U = 0.34 $Å^2$ for O atoms, U = 0.20 $Å^2$ for the methyl groups and U = 0.17 $Å^2$ for the remaining atoms. These were approximately average values of those obtained in the previous calculations.

The *R* value became slightly higher (0.079) because the temperature factors were fixed, but the refinement reached convergence and the DCA geometry remained quite unchanged. The final values of the occupancy factors were close to 0.2 and 0.3 for *A* and *B*, respectively. These values were used in the last refinement cycles and kept fixed while the temperature factors were allowed to change. The *R* value became 0.075, the values of the displacement factors of *B* became stable at the end of the refinement, and more similar to those of model *A*.

The standard deviations on the refined parameters were lower by *ca* 15% and distances and angles for DCA (Table 5, deposited material) were nearer to the expected ones than those obtained at the end of the refinement with single models.

A difference Fourier synthesis showed a residual positive electron density on average lower compared with the equivalent map calculated at the end of the refinement with single models, and the highest value of 0.27 e $Å^{-3}$ corresponded to the C9 methyl-group position of model *C*. However, the electron-density distribution of the camphor region did not allow a three-model refinement. In fact, we did, for the sake of completeness, make a refinement with the *A* + *B* + *C* models, each of weight 1/6, but, as expected, the results were not satisfactory and, in particular, it was not possible to attach any physical meaning to the values of the displacement factors. The *R* value did not decrease (new R = 0.077), the geometry of the DCA remained unchanged and the standard deviations on the parameters were slightly worse (~5% higher).

Therefore, although it is not possible to discard the presence of all the positions corresponding to the potential-energy minima in the crystals, the structure that 'best fits' the experimental data corresponds to the one obtained at the end of the refinement with the models *A* + *B* with occupation factors 0.2 and 0.3, respectively.

In Table 5 the final coordinates for the non-H atoms are reported together with the displacement factors U_{eq} [= $1/3(U_{11} + U_{22} + U_{33})$] for DCA and U_{iso} for LCP. H-atom coordinates and their displacement factors as well as the anisotropic displacement factors of DCA have been deposited (Tables 3 and 4, deposited material). Distances and angles for DCA have also been deposited (Table 5, deposited material). The molecule has a good geometry, similar to that of DCADCP.

At the end of the refinement we recalculated the energy minima of camphor with respect to the final coordinates of DCA. The new values of the rotational and translational parameters as well as the new values of the energy minima were very similar to the previous ones, the maximum deviations being 2°, 0.1 Å and 0.8 kJ mol^{-1}. We also calculated the corresponding new intermolecular DCA–LCP distances which did not show any relevant variation. Therefore, the previous considerations based on potential-energy calculations remain valid for the refined structure.

Discussion

We examined the regions around the three best minima, to check how confined the molecules were within the channels, and calculated the potential energy as a function of the translation in the *ab* plane (Fig. 5) and along

Table 5. *Final fractional atomic coordinates* ($\times 10^4$) *and displacement parameters* ($Å^2 \times 10^3$) *of DCA and LCP molecules*

Standard deviations are in parentheses

$U_{eq} = (1/3)\sum_i \sum_j U_{ij} a_i^* a_j^* \mathbf{a}_i.\mathbf{a}_j$.

	x	y	z	U_{eq}
DCA				
C1	−1312 (2)	1878 (4)	−6139 (8)	59 (3)
C2	−1815 (2)	2229 (4)	−5546 (9)	59 (3)
C3	−1765 (2)	2920 (4)	−3970 (9)	62 (3)
C4	−1486 (2)	2460 (4)	−2381 (9)	61 (3)
C5	−984 (2)	2073 (4)	−2940 (9)	57 (3)
C6	−707 (2)	1615 (4)	−1354 (9)	71 (4)
C7	−929 (3)	643 (4)	−755 (9)	71 (4)
C8	−971 (2)	−59 (4)	−2368 (8)	55 (3)
C9	−1259 (2)	414 (4)	−3991 (8)	49 (2)
C10	−1014 (2)	1371 (4)	−4643 (8)	51 (3)
C11	−1366 (2)	−307 (4)	−5507 (7)	51 (3)
C12	−1610 (2)	−1236 (4)	−4871 (7)	49 (3)
C13	−1305 (2)	−1727 (4)	−3315 (8)	48 (3)
C14	−1224 (2)	−985 (4)	−1791 (8)	52 (3)
C15	−1011 (3)	−1567 (4)	−177 (10)	77 (4)
C16	−1271 (3)	−2544 (5)	−309 (9)	79 (4)
C17	−1543 (2)	−2557 (4)	−2213 (7)	51 (3)
C18	−812 (2)	−2068 (4)	−4199 (10)	60 (2)
C19	−500 (2)	1184 (5)	−5442 (10)	68 (4)
C20	−1541 (2)	−3588 (4)	−3068 (9)	60 (3)
C21	−1802 (2)	−3650 (4)	−4884 (9)	69 (4)
C22	−1729 (2)	−4363 (4)	−1702 (10)	69 (4)
C23	−2253 (2)	−4252 (5)	−1109 (11)	84 (4)
C24	−2405 (2)	−5039 (4)	258 (9)	67 (3)
O25	−2249 (2)	3216 (3)	−3408 (7)	83 (2)
O26	−2096 (1)	−1024 (3)	−4188 (5)	59 (2)
O27	−2365 (3)	−5887 (4)	−61 (8)	123 (5)
O28	−2588 (2)	−4733 (3)	1756 (7)	80 (3)
LCP				
A				
C1	−131 (10)	4966 (19)	985 (30)	224 (7)
C2	39 (10)	3970 (19)	449 (30)	112 (6)
C3	95 (10)	3374 (19)	2177 (30)	163 (7)
C4	−43 (10)	4129 (19)	3671 (30)	191 (7)
C5	−594 (10)	4259 (19)	3553 (30)	199 (7)
C6	−664 (10)	4811 (19)	1701 (30)	148 (7)
C7	150 (10)	5086 (19)	2853 (30)	211 (7)
C8	712 (10)	5124 (19)	2586 (30)	124 (6)
C9	−3 (10)	6003 (19)	3960 (30)	238 (7)
C10	−82 (10)	5724 (19)	−470 (30)	161 (7)
O	103 (10)	3743 (19)	−1105 (30)	325 (7)
B				
C1	−40 (6)	5267 (10)	3015 (18)	143 (6)
C2	487 (6)	5163 (10)	3608 (18)	166 (6)
C3	799 (6)	5011 (10)	1915 (18)	196 (6)
C4	399 (6)	5015 (10)	386 (18)	152 (6)
C5	239 (6)	6053 (10)	167 (18)	188 (6)
C6	−54 (6)	6254 (10)	1971 (18)	140 (6)
C7	−47 (6)	4552 (10)	1350 (18)	79 (5)
C8	32 (6)	3494 (10)	1962 (18)	164 (6)
C9	−531 (6)	4587 (10)	201 (18)	171 (6)
C10	−415 (6)	5169 (10)	4509 (18)	202 (7)
O	609 (6)	5214 (10)	5170 (18)	379 (7)

the channel (z direction) (Fig. 6). In agreement with the large number of good interactions for each minimum, the possible movement of the molecule in the *ab* plane is small for all of them. Moreover, the energy gradient along the z direction (Fig. 6) is similar to that on the *ab* plane, indicating that the camphor molecules cannot easily escape along the channels. This is due to the slightly hourglass shape of the channels (Fig. 7).

The same type of interaction, both in nature and in number, were found for the DCADCP crystals for which the energy values of the minima ranged between −107.0 and −100.3 kJ mol^{-1} (−106.6 and −102.8 kJ mol^{-1} in the present work). Further, the O atom of LCP and the C_6H_2 group, which exchange positions in the two isomers, are not involved in any strong interaction in either structure. From this comparative picture it is to be expected that the DCA lattice is not capable of an efficient enantiomeric

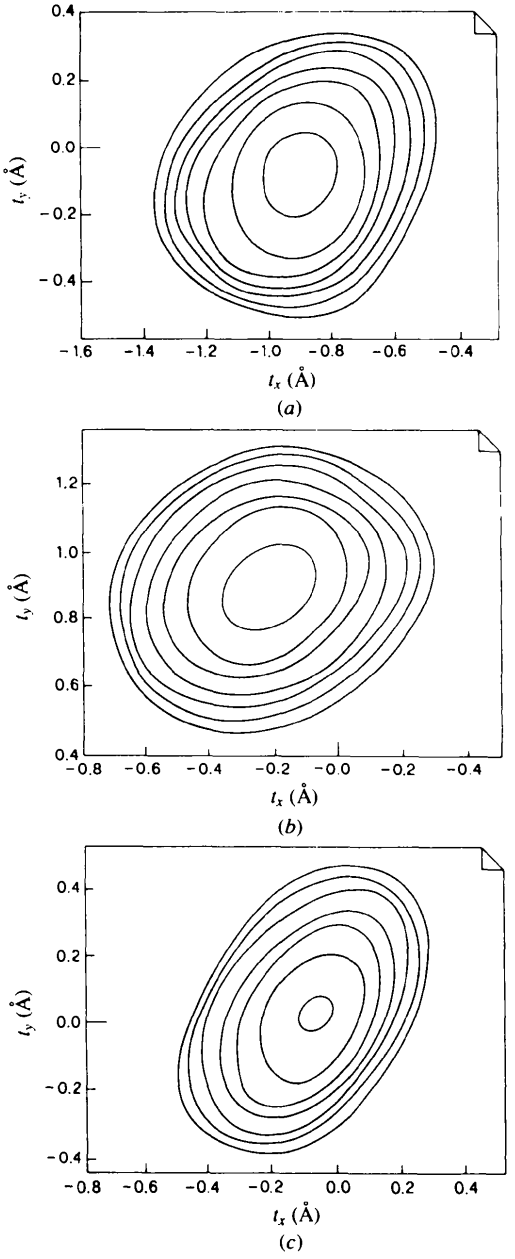

Fig. 5. van der Waals energy of LCP as a function of the translations t_x and t_y in the region of the three deepest minima. Contour lines at intervals of 2.1 kJ mol^{-1} starting from −92 kJ mol^{-1}.

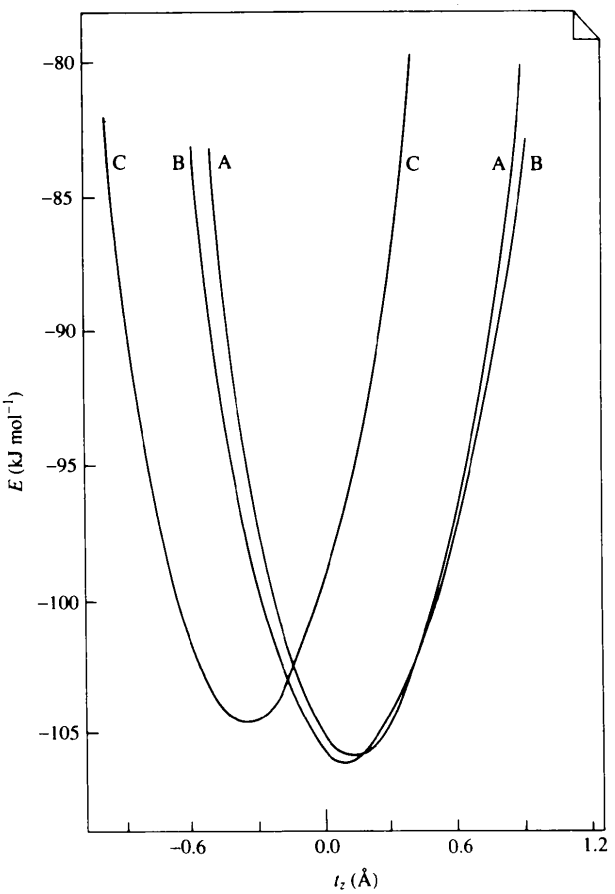

Fig. 6. van der Waals energy of LCP as a function of the translation t_z in the region of the three deepest minima.

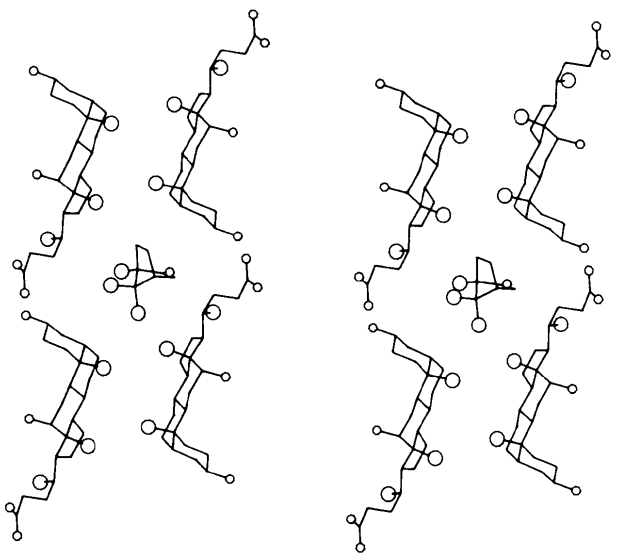

Fig. 7. Stereoscopic view of the DCALCP structure in the region of the channel. The LCP position is that corresponding to the energy minimum *B* at the end of the refinement. Small circles represent O atoms, large circles represent methyl groups. H atoms are omitted.

discrimination in the case of camphor. This is also supported by some qualitative measurements of the vapour pressure of DCADCP and DCALCP crystals as a function of the temperature (V. Piacente, private communication) carried out with the torsion–effusion method (Piacente, Pompili, Scardala & Ferro, 1991), showing that the behaviour of the two crystals was very similar. For both crystals the release of the camphor molecules gave rise to enthalpy changes very low and not appreciably different from each other. This is at variance with the behaviour of DCA inclusion compounds containing aromatic molecules, like DCA–styrene (57 kJ mol^{-1}) and DCA–phenanthrene (129 kJ mol^{-1}) where strong interactions are formed between the methyl groups and H atoms of DCA and the π-cloud of the guest molecules (Giglio, 1984, and references therein).

Although many orthorhombic crystal structures of DCA have been studied, only few are known where the cavity has the same geometry as that found in DCALCP crystals, therefore, there is still need for further investigation.

In more recent years molecular recognition properties are also reported for the inclusion compounds of cholic acid [3α,7α,12α-trihydroxy-5β-cholan-24-oic acid (Lessinger, 1982; Jones & Nassimbeni, 1990; Miyata *et al.*, 1990)]. For this bile acid the cavity flexibility is attained through variation of the side-chain conformation, while for DCA the side-chain conformation is almost identical in all the orthorhombic crystals. However, both deoxycholic and cholic acid are small molecules capable of a high degree of molecular recognition through the formation of stable molecular aggregates of macromolecular size. This important property is common to the salts of the bile acids, the aggregates of which are responsible for their biological functions, through the interactions with biomolecules of the physiological medium (Reisinger & Lightner, 1985; Campanelli *et al.*, 1989; D'Alagni, Delfini, Galantini & Giglio, 1992).

There are many aspects of the activity of these compounds that still have to be clarified. For this purpose a systematic study of their aggregation schemes and interactions in the solid state and in solution needs to be carried out.

The authors thank Professor V. Piacente for the vapour-pressure measurements, Professor E. Giglio for useful discussions and the Italian MURST (Ministero per l'Universita' e la Ricerca Scientifica e Tecnologica) and CNR (Consiglio Nazionale delle Ricerche) for financial support.

References

ANGELICO, M., CANDELORO DE SANCTIS, S., GANDIN, C. & ALVARO, D. (1990). *Gastroenterology*, **98**, 444–453.

AUDISIO, G., SILVANI, A. & ZETTA, L. (1984). *Macromolecules*, **17**, 29–32.

BAERT, F. & FOURET, R. (1978). *Acta Cryst.* B**34**, 2546–2551.

BARON, M. (1961). *Phys. Methods Chem. Anal.* **4**, 223–266.

CAMPANELLI, A. R., CANDELORO DE SANCTIS, S., CHIESSI, E., D'ALAGNI, M., GIGLIO, E. & SCARAMUZZA, L. (1989). *J. Phys. Chem.* **93**, 1536–1542.
CANDELORO DE SANCTIS, S. & GIGLIO, E. (1979). *Acta Cryst.* B**35**, 2650–2655.
CANDELORO DE SANCTIS, S., CHIESSI, E. & GIGLIO, E. (1985). *J. Incl. Phenom.* **3**, 55–64.
CANDELORO DE SANCTIS, S., COIRO, V. M., GIGLIO, E., PAGLIUCA, S., PAVEL, N. V. & QUAGLIATA, C. (1978). *Acta Cryst.* B**34**, 1928–1933.
CANDELORO DE SANCTIS, S., GIGLIO, E., PAVEL, V. & QUAGLIATA, C. (1972). *Acta Cryst.* B**28**, 3656–3661.
CANDELORO DE SANCTIS, S., GIGLIO, E., PETRI, F. & QUAGLIATA, C. (1979). *Acta Cryst.* B**35**, 226–228.
COIRO, V. M., D'ANDREA, A. & GIGLIO, E. (1979). *Acta Cryst.* B**35**, 2941–2944.
COIRO, V. M., GIGLIO, E., MAZZA, F. & PAVEL, N. V. (1984). *J. Incl. Phenom.* **1**, 329–337.
CRAVEN, B. M. & DE TITTA, G. T. (1972). *J. Chem. Soc. Chem. Commun.* pp. 530–531.
CROMER, D. T. & MANN, J. B. (1968). *Acta Cryst.* A**24**, 321–324.
D'ALAGNI, M., DELFINI, M., GALANTINI, L. & GIGLIO, E. (1992). *J. Phys. Chem.* **96**, 10520–10528.
GAVUZZO, E., PAGLIUCA, S., PAVEL, N. V. & QUAGLIATA, C. (1972). *Acta Cryst.* B**28**, 1968–1969.
GIACOMELLO, G. & KRATKY, O. (1936). *Z. Kristallogr. A*, **95**, 459–464.
GIGLIO, E. (1984). *Inclusion Compounds*, Vol. 2, edited by J. L. ATWOOD, J. E. D. DAVIES & D. D. MCNICOL, ch. 7, pp. 207–229. London: Academic Press.
HIGUCHI, W. I. (1984). *Hepatology*, **4**, 161S–165S.
HOLZBACH, R. T. (1984). *Hepatology*, **4**, 173S–176S.
HOSTROW, J. D. (1984). *Hepatology*, **4**, 215S–222S.
JONES, E. L. & NASSIMBENI, L. R. (1990). *Acta Cryst.* B**46**, 399–405.
JONES, J. G., SCHWARZBAUM, S., LESSINGER, L. & LOW, B. W. (1982). *Acta Cryst.* B**38**, 1207–1215.
LESSINGER, L. (1982). *Cryst. Struct. Commun.* **11**, 1787–1792.
MAKIN, E. C. (1975). *New Developments in Separation Methods*, edited by E. GRUSHKA, pp. 49–64. New York/Basel: Marcel Dekker.
MIKI, K., KASAI, N., TSUTSUMI, H., MIYATA, M. & TAKEMOTO, K. (1987). *J. Chem. Soc. Chem. Commun.* pp. 545–546.
MIYATA, M. & TAKEMOTO, K. (1975). *Polymer Lett.* **13**, 221–223.
MIYATA, M., SHIBAKAMI, M., CHIRACHANCHAI, S., TAKEMOTO, K., KASAI, N. & MIKI, K. (1990). *Nature (London)*, **343**, 446–447.
PADMANABHAN, K., VENKATESAN, K. & RAMAMURTHY, V. (1984). *Can. J. Chem.* **62**, 2025–2028.
PADMANABHAN, K., VENKATESAN, K. & RAMAMURTHY, V. (1987). *J. Incl. Phenom.* **5**, 315–323.
PAVEL, N. V., QUAGLIATA, C. & SCARCELLI, N. (1976). *Z. Kristallogr.* **144**, 64–75.
PIACENTE, V., POMPILI, T., SCARDALA, P. & FERRO, D. (1991). *J. Chem. Thermodynam.* **23**, 379–396.
POPOVITZ-BIRO, R., TANG, C. P., CHANG, H. C., LAHAV, M. & LEISEROWITZ, L. (1985). *J. Am. Chem. Soc.* **107**, 4043–4058.
REISINGER, M. & LIGHTNER, D. A. (1985). *J. Inclusion Phenom.* **3**, 479–485.
SHELDRICK, G. M. (1976). *SHELX76. Program for Crystal Structure Determination.* Univ. of Cambridge, England.
TANG, C. P., POPOVITZ-BIRO, R., LAHAV, M. & LEISEROWITZ, L. (1979). *Isr. J. Chem.* **18**, 385–389.
WEISINGER-LEWIN, Y., VAIDA, M., POPOVITZ-BIRO, R., CHANG, H. C., MANNIG, F., FROLOW, F., LAHAV, M. & LEISEROWITZ, L. (1987). *Tetrahedron*, **43**, 1449–1475.
WIELAND, H. & SORGE, H. (1916). *Z. Physiol. Chem.* **97**, 1–27.

Acta Cryst. (1995). B**51**, 89–98

Structure of Ureido-Balhimycin

BY GEORGE M. SHELDRICK

Institut für Anorganische Chemie der Universität Göttingen, Tammannstrasse 4, *D*-37077 *Göttingen, Germany*

ERICH PAULUS* AND LÁSZLÓ VÉRTESY

Hoechst AG, D-65926 *Frankfurt am Main, Germany*

AND FRIEDEMANN HAHN

Stoe & Cie GmbH, Hilpertstrasse 10, *D*-64295 *Darmstadt, Germany*

(*Received* 17 *March* 1994; *accepted* 6 *September* 1994)

Abstract

The structure of the ureido derivative of balhimycin has been solved by Patterson vector superposition followed by iterative partial structure expansion, and refined against F^2 to R_1 = 0.0536 for 8949 $F > 4\sigma(F)$ and 0.0802 for all 11 977 image plate data. Crystal data: $C_{67}H_{74}Cl_2N_{10}O_{25}.27.75(H_2O)$, M_r = 1990.20, triclinic, $P1$, a = 17.909 (10), b = 18.466 (10), c = 18.873 (13) Å, α = 96.65 (5), β = 114.15 (5), γ = 114.78 (4)°, V = 4850 (5) Å^3, Z = 2, D_x = 1.363 Mg m^{-3}, Mo $K\alpha$, λ = 0.71073 Å, μ = 0.17 mm^{-1}, $F(000)$ = 2115, T = 293 K. This appears to be the first reported crystal structure of a naturally occuring member of the vancomycin family which has not been subject to degradation and ring rearrangement, and it appears likely that the conformation observed is close to that required for complex formation with cell-wall protein. It possesses a 'binding pocket' for the C-terminal carboxyl of this protein, which is consistent with suggestions based on NMR data. The two antibiotic molecules in the unit cell are bound by antiparallel hydrogen bonds to form a tight dimer, which may well persist in biological systems.

* Author to whom correspondence should be addressed.